Technical Notes

TECHNICAL NOTES are short manuscripts describing new developments or important results of a preliminary nature. These Notes cannot exceed 6 manuscript pages and 3 figures; a page of text may be substituted for a figure and vice versa. After informal review by the editors, they may be published within a few months of the date of receipt. Style requirements are the same as for regular contributions (see inside back cover).

Flow Generated by an Array of Eccentric Porous Tubes

Kwok-On Tong,* Charles J. Knight,† and Joel M. Avidor‡
Avco Everett Research Laboratory, Inc., Everett, Mass.

I. Introduction

THE average output power of a multiple-pulsed laser device depends not only on the per-pulse energy but also on the pulse repetition frequency. In devices utilizing gas flow as lasing medium, the maximum pulse repetition rate depends on the time required to remove the processed gas out of the lasing region. In the present study, our attention is directed toward the case of an electric discharge laser in which the gas flow is generated by injecting gas through a parallel grid of porous tubes. This particular scheme has been studied previously with uniform injection around the circumference of each porous tube, i.e., porous tubes with uniform cross section.[1] It was observed that the flow generated by such porous tubes is strongly wakelike. This means that the time required to remove the processed gas out of the lasing region is substantially longer than the time required if the flow were uniform. Such inefficiency in mass utilization can be reduced by using porous tubes with a cross section of circular inner and outer contours with displaced centers.

II. Porous Tube with Nonuniform Injection

A. Ideal Normal Velocity Distribution

In Ref. 1, an inviscid rotational flow model was used to analyze the wakelike flowfield generated by an array of concentric porous tubes. Such wakelike behavior can be avoided only if the flow is irrotational. Streamlines must issue normal to the tubes as the pressure drop across the porous material is large compared to the dynamic pressure. Therefore, since only one boundary condition is permitted for irrotational flow, this flowfield is obtained by solving Laplace's equation for the stream function, subject to the no-slip condition.[2] Figure 1 shows the resulting ideal velocity distribution at the tube surface for a particular array of 0.95-cm o.d. porous tubes with 2.54 cm tube spacing. Note that it is circumferentially nonuniform. Here $\bar{u}_n$ is the average normal velocity around the circumference of each tube and θ is the angular location on the tube surface.

B. Flow Through Porous Tube Walls

The porous tubes operate in a regime where both viscous- and inertia-dominated permeabilities are important. A reasonable constitutive relation for the velocity normal to an isobar in the porous media is

$$\alpha\mu u_n + \beta\rho u_n^2 = -\frac{dp}{dn} \tag{1}$$

where the directional derivative is along a unit vector, n, normal to the isobar and pointed in the flow direction. The parameters α and β are material constants and μ is the first coefficient of viscosity. Combining Eq. (1) with the assumption of an isothermal isotropic porous medium, the perfect gas law, and the compressible continuity equation, the equation for the pressure in the porous media can be obtained as[2]

$$\text{div}(k\ \text{grad}\ p^2) = 0 \tag{2}$$

where

$$k = \left(-\frac{\alpha\mu}{2\beta} + \sqrt{\left(\frac{\alpha\mu}{2\beta}\right)^2 + \frac{|\text{grad}\ p^2|}{2\beta RT}}\right) \Big/ |\text{grad}\ p^2|$$

and R is the gas constant.

In principle, one could design the wall thickness distribution of a porous tube to match the ideal normal velocity distribution using Eqs. (1) and (2). However, there are practical considerations in manufacturing porous tubes with nonconcentric cross section. The cross section of eccentric circular inner and outer contours seems to provide a more practical solution.

The velocity distribution on the outer surface of an eccentric porous tube can be obtained by solving Eq. (2), with the condition that the inner and outer circular contours are isobars. A closed-form solution can be obtained for the case of $k = \text{const}$[2] which corresponds to viscous-dominated flow. This is shown as the dotted line on Fig. 1 for an eccentric porous tube with 0.95 cm o.d., 0.64 cm i.d. and 0.11 cm thin wall thickness. In the curve form shown in Fig. 1, the velocity distribution is a strong function of the eccentricity of the tube cross section only. On the other hand, the average normal velocity $\bar{u}_n$ depends strongly on α, β, the pressure inside the tube, and the difference between the radii of the outer and inner circular contours.

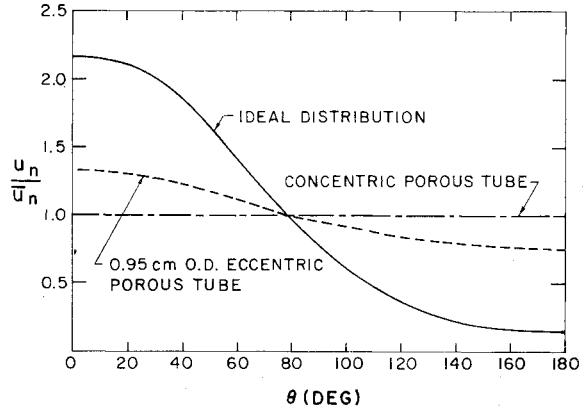

Fig. 1 Normal velocity distributions for ideal case and an 0.95 cm o.d. eccentric porous tube.

Presented as Paper 77-662 at the AIAA 10th Fluid and Plasmadynamics Conference, Albuquerque, N. Mex., June 27-29, 1977; submitted Nov. 21, 1977; revision received March 16, 1978.

Index categories: Jets, Wakes, and Viscid-Inviscid Flow Interactions; Subsonic Flow; Lasers.

*Senior Scientist. Member AIAA.
†Principal Research Scientist. Member AIAA.
‡Principal Research Scientist; presently with SOREQ Research Center, Israel. Member AIAA.

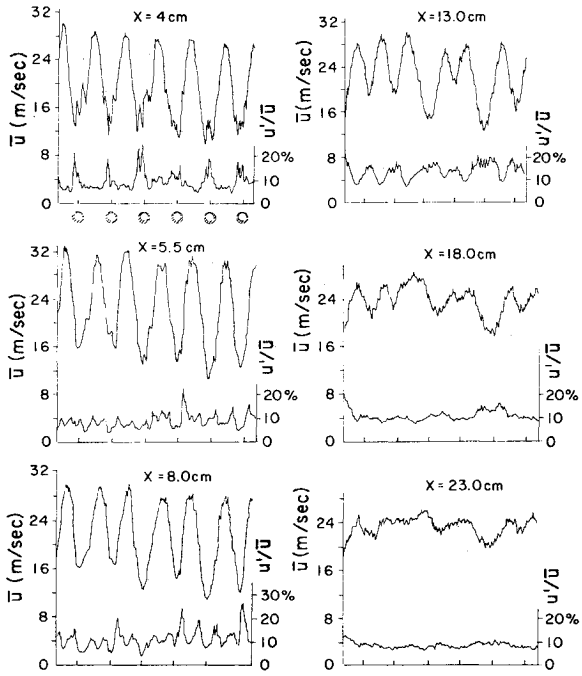

Fig. 2 Flowfield downstream of an array of eccentric porous tubes.

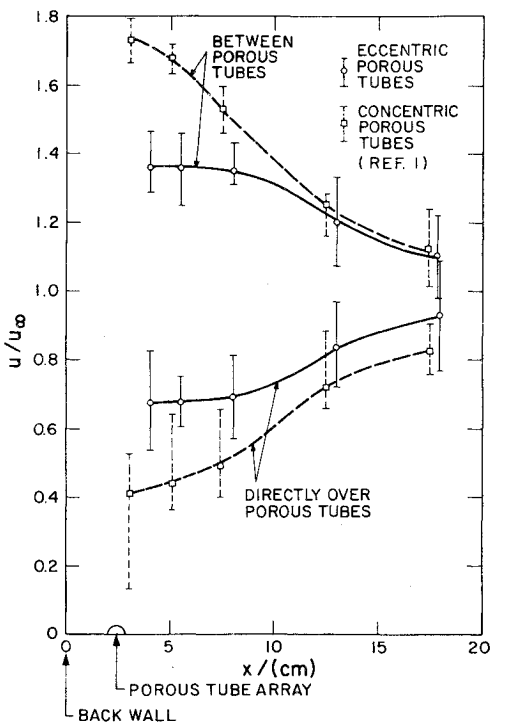

Fig. 3 Comparison of the wake-like flowfields generated by eccentric and concentric porous tubes.

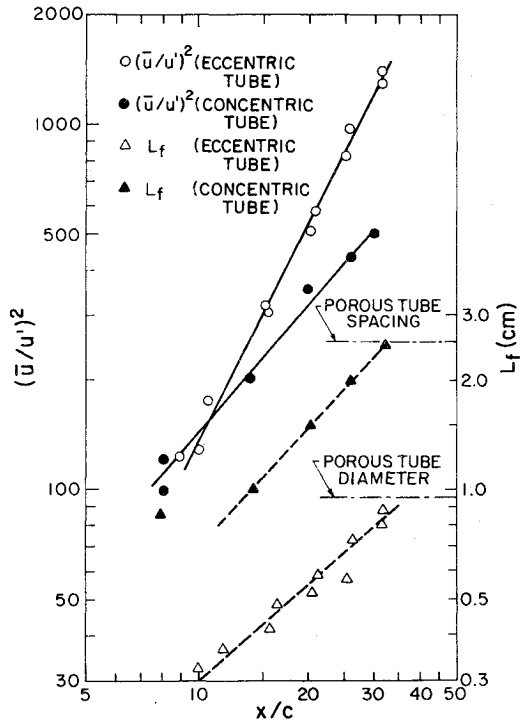

Fig. 4 Decay of turbulent energy and distribution of longitudinal scale size.

III. Experiments and Results

The eccentric porous tubes used in the present study have average dimensions of 0.95-cm o.d., 0.62-cm i.d., 0.11-cm thin wall thickness and 35.6-cm length. These sintered stainless steel tubes have very low porosity to insure a large pressure drop across the tube wall and therefore a uniform mass injection rate along the tube length. The porous tubes were arranged in a parallel grid with 2.54-cm tube spacing and connected to two 5-cm i.d. pipes serving as flow source plenum.[1] This porous tube array was then enclosed in a five-sided plexiglas enclosure to prevent entrainment of ambient air into the near-field of the porous tube-generated flow. The thick wall of each tube was placed facing the bottom plate located 2.54 cm below the grid. Compressed nitrogen was supplied to the flow source plenum through a dome regulator to insure constant plenum pressure during each test run. A constant temperature hot-wire anemometer system and a true rms voltmeter (Thermo-Systems, Inc.) were used for velocity and turbulent intensity measurements.

The distributions of mean velocity ($\bar{u}$) and turbulent intensity ($u'/\bar{u}$) were measured at different locations downstream of the grid and are shown in Fig. 2. Here x is measured from the bottom plate of the enclosure. In general, the flowfield displays a wakelike behavior with a decrease in velocity over the porous tubes, similar to the flow generated by an array of concentric porous tubes.[1] Variations do exist between different wakes, presumably caused by the imperfect orientation and geometry of each eccentric tube and nonuniformities in the injection through different tubes. The nonuniformities in mean velocity and turbulent intensity distributions decay rapidly, and at $x=23$ cm they approach uniformity.

Figure 3 is a comparison between the flowfields generated by the eccentric porous tubes array and a similar array of 0.95-cm o.d. concentric porous tubes. It shows the measured maximum velocity (between porous tubes) and minimum velocity (directly over porous tubes) at different locations. u_∞ is the average flow speed far downstream of the tube array. Even with the large scatter in both sets of data, the eccentric porous tube generated flow shows large reduction in velocity defect, especially near the tube grid, which significantly improves the effectiveness in mass utilization. For the eccentric porous tube generated flowfield (Fig. 2), the time required to remove the slowest moving fluid from the region bounded by the exterior x location of the thin wall section and $x=23$ cm is approximately 1.4 times the time needed if the entire flow were uniform. The flowfield generated by a similar array of concentric porous tubes would require a flow removal time twice that needed for a uniform flowfield.

The decay of turbulent energy $[(u'/\bar{u})^2]$ and the longitudinal integral scale size (L_f) have also been measured in the far-field to determine whether the eccentric porous

tube-generated flow possesses the characteristics of isotropic turbulence far enough downstream of the tube array as in the case of concentric porous tube array.[1] The results are shown in Fig. 4, with c being the tube spacing. The turbulent energy in both cases is roughly the same at eight tube spacings from the tube grid (i.e., $x/c \approx 9$). The eccentric tube data show that the turbulent energy decays thereafter as $(x/c)^{-2}$, which is different from the $(x/c)^{-1.1}$ dependence observed by Avidor,[1] Gas-El-Hak,[3] and Tassa.[4] Based on Taylor's hypothesis of frozen convection, the scale size was computed from the measured average velocity and autocorrelations using the relation $L_f = u\int_0^\infty R(\tau)\,d\tau$. The eccentric porous tube data show a substantially smaller scale size which increase approximately as $(x/c)^{0.9}$, slightly different from the linear increase observed in the concentric tube-generated flow.

Acknowledgment

This work was supported by Naval Research under Contract No. N00014-76-C-0040.

References

[1] Avidor, J. M., Kemp, N. H., and Knight, C. J., "Experimental and Theoretical Investigation of Flow Generated by an Array of Porous Tubes," *AIAA Journal*, Vol. 14, Nov. 1976, pp. 1534-1540.

[2] Tong, K.-O, Knight, C. J., and Avidor, J. M., "Flow Generated by an Array of Eccentric Porous Tubes," AIAA Paper 77-662, Albuquerque, N. Mex., 1977.

[3] Gad-El-Hak, M. and Corrsin, S., "Measurements of Nearly Isotropic Turbulence Behind a Uniform Jet Grid," *Journal of Fluid Mechanics*, Vol. 62, Jan. 1974, pp. 115-143.

[4] Tassa, Y. and Kamotani, Y., "Experiments on Turbulence Behind a Grid with Jet Injection in Downstream and Upstream Direction," *The Physics of Fluids*, Vol. 18, April 1975, pp. 411-414.

Numerical Method for Boundary Layers with Blowing—The Exponential Box Scheme

T. M. El-Mistikawy* and M. J. Werle†
University of Cincinnati, Cincinnati, Ohio

Introduction

NUMERICAL solutions of boundary-layer flows in the presence of massive injection through a porous surface are complicated by the multistructure nature of the flowfield. This Note presents a new numerical scheme based on exponential difference operator concepts,[1-5] combined with Keller's box scheme approach[6] to produce a stable second-order accurate finite-difference scheme for such convection-diffusion problems. The technique developed here is demonstrated through application to the self-similar boundary-layer equations with massive blowing at the surface.

Governing Equations and Solution Method

Attention here is directed toward solution of the Falkner-Skan equations with blowing given here as

$$V_\eta + F = 0, \quad F_{\eta\eta} - VF_\eta + \beta(1 - F^2) = 0 \tag{1}$$

with

$$F(0) = 0, \quad V(0) = V_w, \quad F \to 1 \text{ as } \eta \to \infty \tag{2}$$

where V_w is related to the physical injection velocity, F represents the normalized longitudinal velocity component, and β the inviscid pressure-gradient parameter.

In the present study, an iterative numerical approach is used to first write the momentum equation as

$$F_{\eta\eta} - (a+b)F_\eta + abF = -\beta \tag{3}$$

where a and b are assumed to be known from a previous iteration and are given as

$$a \equiv V/2 + \sqrt{(V/2)^2 + \beta F}, \quad b \equiv V/2 - \sqrt{(V/2)^2 + \beta F} \tag{4}$$

A departure is now made from the classical approach of solving Eq. (3) using Taylor's series to generate difference approximations to derivatives over a small grid distance. Following the lead of Refs. 1-5, the coefficients of Eq. (3) are first approximated over each small grid distance by constants, and the resulting equation integrated exactly. The resulting solution between points 1 and 2 of Fig. 1 is:

$$F_{1,2} = A_1 e^{a_1\eta} + B_1 e^{b_1\eta} + f_1 \tag{5}$$

where $f_1 \equiv -\beta/a_1 b_1$, and the coefficients a_1, b_1 are evaluated at the midpoint of the grid indicated. Use of Eq. (5), a similar expression for $F_{2,3}$ in the interval between points 2 and 3, and the two continuity conditions that $F_{2+} = F_{2-}$ and $F_{\eta 2+} = F_{\eta 2-}$ produce the difference relation

$$r_1 F_1 - (s_1 + s_2)F_2 + r_2 F_3 = (r_1 - s_1)f_1 + (r_2 - s_2)f_2 \tag{6}$$

where

$$r_1 = (a_1 - b_1)e^{b_1\Delta\eta_1}/t_1, \quad r_2 = (a_2 - b_2)e^{-a_2\Delta\eta_2}/t_2 \tag{7a}$$

$$s_1 = [a_1 - (1 - t_1)b_1]/t_1, \quad s_2 = [a_2(1 - t_2) - b_2]/t_2 \tag{7b}$$

$$t_1 = 1 - e^{-(a_1 - b_1)\Delta\eta_1}, \quad t_2 = 1 - e^{-(a_2 - b_2)\Delta\eta_2} \tag{7c}$$

Equation (6) is a three-point difference approximation to Eq. (3) that produces an easily solvable tridiagonal set of algebraic equations. In addition, it possesses all the favorable properties of both the exponential and "two-point" or "box" scheme approaches (Ref. 6). It is found to be diagonally dominant for $ab < 0$, it is second-order accurate in $\Delta\eta_i$ throughout the diffusion region, and most important, it automatically and smoothly switches to a second-order accurate windward difference scheme as the normal convection velocity V (as represented by the term $a+b$) becomes large, negative or positive.

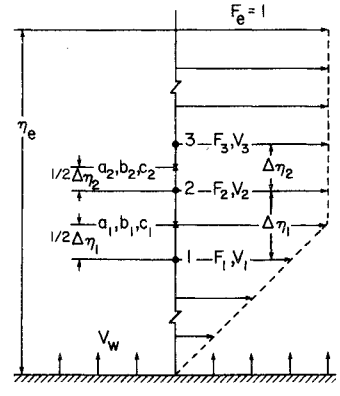

Fig. 1 Nomenclature and grid geometry.

Received Nov. 22, 1977; revision received March 21, 1978.

Index categories: Boundary Layers and Convective Heat Transfer—Laminar; Computational Methods.

*Graduate Research Assistant, Dept. of Aerospace Engineering and Applied Mechanics.

†Professor, Dept. of Aerospace Engineering and Applied Mechanics; currently Chief, Gas Dynamics Section, United Technologies Research Center, East Hartford, Conn. Member AIAA.